RAA 2014 Vol. **14** No. **1**, 104–112 doi: 10.1088/1674–4527/14/1/009
http://www.raa-journal.org *http://www.iop.org/journals/raa*

Research in Astronomy and Astrophysics

Low-dimensional chaos and fractal properties of long-term sunspot activity *

Shuang Zhou[1,2], Yong Feng[1], Wen-Yuan Wu[1], Yi Li[1] and Jiang Liu[1]

[1] Chongqing Key Laboratory of Automated Reasoning and Cognition, Chongqing Institute of Green and Intelligent Technology, Chinese Academy of Sciences, Chongqing 400714, China; *zhoushuang@cigit.ac.cn*

[2] University of Chinese Academy of Sciences, Beijing 100049, China

Received 2013 July 31; accepted 2013 August 18

Abstract Two primary solar-activity indicators− sunspot numbers (SNs) and sunspot areas (SAs) in the time interval from November 1874 to December 2012 − are used to determine the chaotic and fractal properties of solar activity. The results show that (1) the long-term solar activity is governed by a low-dimensional chaotic strange attractor, and its fractal motion shows a long-term persistence on large scales; (2) both the fractal dimension and maximal Lyapunov exponent of SAs are larger than those of SNs, implying that the dynamical system of SAs is more chaotic and complex than SNs; (3) the predictions of solar activity should only be done for short- to mid-term behaviors due to its intrinsic complexity; moreover, the predictability time of SAs is obviously smaller than that of SNs and previous results.

Key words: methods: data analysis — Sun: activity — Sun: sunspots

1 INTRODUCTION

It is well known that sunspot numbers (SNs) and sunspot areas (SAs) are two direct indicators of solar activity that are widely and frequently used to describe long-term solar variability (Li et al. 2009; Feng et al. 2013; Deng et al. 2013a,b,c). These two time series are also used to deal with the question of whether solar activity and the underlying dynamo mechanism have a periodic, chaotic or stochastic nature (Hanslmeier 1997; Hanslmeier & Brajša 2010; Hanslmeier et al. 2013; Usoskin 2013). Unfortunately, it has not been clear whether the solar dynamo behaves like a chaotic or a stochastic system, although nonlinear effects in astrophysics and cosmology have been studied in theoretical models and reviewed by several authors (Feynman & Gabriel 1990; Schmalz & Stix 1991; Mundt et al. 1991; Kremlyovskij et al. 1992; Rozelot 1995; Tobias 1996; Zhang 1998; Jevtić et al. 2001; Li & Li 2007a,b; Greenkorn 2009). However, several authors found no evidence that the sunspots are generated by a low-dimensional chaotic process (Price et al. 1992; Carbonell et al. 1994; Charbonneau & Dikpati 2000; Mininni et al. 2002). Actually, there are two possible reasons that can cause different results. On one hand, the observational data used in different papers do not have uniform quality; only longer, more reliable data sets with low noise can obtain more accurate results. On the other hand, it is easy to obtain a spurious indication of low-dimensional dynamical

* Supported by the National Natural Science Foundation of China.

chaos in solar activity if the analysis methods are not carried out properly (Panchev & Tsekov 2007). Therefore, it is necessary and timely to re-analyze the chaotic and fractal properties of solar activity with longer, higher quality data sets and proper analysis techniques.

The Lyapunov exponent may judge the degree of chaos inherent in a time series but does not characterize its fractal properties; the Hurst exponent is not only used as a measure of long-term memory but is also related to the fractal dimension of the time series, and it has been used in many fields, such as geology (Carr 1997), geomagnetism (Wanliss & Reynolds 2003), solar activity (Oliver & Ballester 1996) and so on. Furthermore, we will use rescaled range analysis which has good robustness to estimate the Hurst exponent. We will also use principal component analysis to distinguish whether a time series is a chaotic signal or a noisy signal.

Following the rising interest in the study of nonlinear behavior associated with solar activity, the objective of this work is to investigate the chaotic and fractal properties of both SNs and SAs. The remainder of this paper is organized as follows. Section 2 contains a description of the data set and analysis methods employed in this study. Analyses and results are presented in Section 3. Finally Section 4 gives the conclusions and discussion.

2 DATA AND METHODOLOGY

2.1 Description of Data

Continuous time series of monthly-mean SNs and SAs, which have been widely and frequently used to describe long-term solar activity, can be publicly downloaded from the Solar Influences Data Analysis Center's website[1] and the National Aeronautics and Space Administration's website[2]. These two data series should be smoothed before the phase space is reconstructed due to noise in the time series (Kremliovsky 1994). To filter the noise but keep the essential dynamics contained in the two data sets, we employ a 13-point smoothing method to smooth them (Deng et al. 2012a,b). These two examples of data series cover the time interval from November 1874 to December 2012, and both of them are shown in Figure 1.

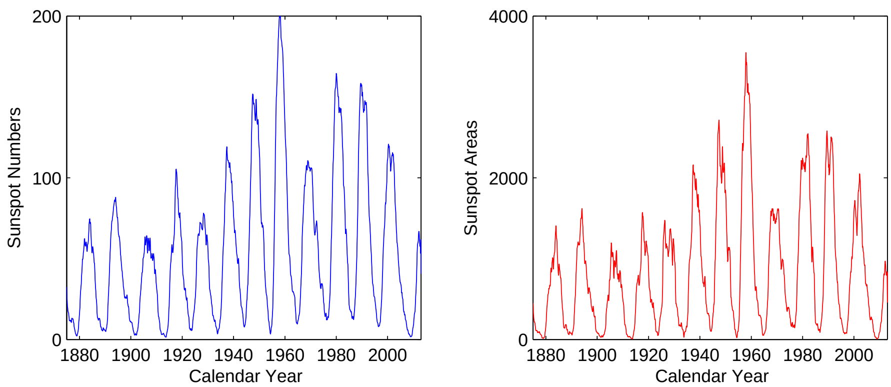

Fig. 1 Plots of the smoothed monthly-mean SNs (*left panel*) and SAs (*right panel*) from November 1874 to December 2012.

[1] *http://sidc.oma.be/sunspot-data/*
[2] *http://solarscience.msfc.nasa.gov/greenwch.shtml*

2.2 Methods of Analysis: Qualitative Methods

2.2.1 Principal Component Analysis

The method of principal component analysis, which was proposed by Karl Pearson, can be used for distinguishing whether a time series is chaotic or not (Gong & Xu 1997). For a time series $x = \{x_1, x_2, \cdots, x_n\}$, the covariance matrix A of x is

$$A = \frac{1}{n - (m-1) \times \tau} X \cdot X^T, \tag{1}$$

where τ is the time delay, m is the embedding dimension, and X is the trajectory matrix of the time series. Subsequently, we calculate the eigenvalues $\lambda = \{\lambda_1, \lambda_2, \cdots, \lambda_m\}$ of A, and the sum of all eigenvalues can be represented as $\lambda_{\rm sum} = \sum_{i=1}^{m} \lambda_i$. Finally, we plot how the principal component $\ln(\frac{\lambda_i}{\lambda})$ varies with i. This plot is called a principal component spectrogram, and if there exists a line with negative slope in the principal component spectrogram, the time series is chaotic. Otherwise, it is a noisy signal.

2.2.2 Phase space portrait

To better understand the underlying dynamics of a scalar time series, we need to reconstruct an m-dimensional phase space (Deng et al. 2013d). Fortunately, Packard et al. (1980) and Takens (1981) provide us with a mathematical way to compose the reconstructed phase space y of a given time series $\{x(t), t = 1, 2, \cdots, n\}$

$$y = \left\{ \begin{array}{cccc} x(1) & x(2) & \cdots & x[n-(m-1)\times\tau] \\ x(1+\tau) & x(2+\tau) & \cdots & x[n-(m-2)\times\tau] \\ \cdots & \cdots & \cdots & \cdots \\ x[1+(m-1)\times\tau] & x[2+(m-1)\times\tau] & \cdots & x(n) \end{array} \right\} \tag{2}$$

where τ is the time delay and m is the embedding dimension. These two parameters need to be calculated before reconstructing the phase space. Here we use the mean mutual information, which was first proposed by Fraser & Swinney (1986), and the Cao method given by Cao (1997) to calculate reasonable values for these two important parameters, respectively.

The idea of the Cao method is to increase the dimension of the phase space up to the point where there are no longer any self-intersections in the trajectory. To avoid the choice of a threshold to decide whether a neighbor is false or not, Cao defined a quantity $E_1(d)$ – the relative change in the average distance between two neighboring points – when the dimension is increased from d to $d+1$. The embedding dimension is minimized when the relative change in the average distance saturates around 1. Cao also defined another quantity $E_2(d)$ to distinguish deterministic signals from stochastic signals. The future values are independent of the past values for a random data series, so the value of $E_2(d)$ will be equal to 1 for any dimension. However, $E_2(d)$ cannot be constant for all dimensions in a deterministic data set, because it is certainly related to the dimension of the phase space.

2.3 Methods of Analysis: Quantitative Methods

2.3.1 Rescaled range analysis

The Hurst exponent (H) was originally proposed by Hurst (1951) for analyzing stochastic time series. For a discrete time series $x(t)$, the classical method for calculating the value of H is widely known as the rescaled range analysis, which can be described as

$$R(l)/S(l) = c \times l^H, \qquad 0 \leq H \leq 1 \tag{3}$$

and

$$R(l) = \max_{1\le t\le l}\left[\sum_{u=1}^{t}\left(x(u) - \overline{x}_l\right)\right] - \min_{1\le t\le l}\left[\sum_{u=1}^{t}\left(x(u) - \overline{x}_l\right)\right], \tag{4}$$

where $S(l)$ is the standard deviation, c is a constant and l is the length of the segment used in our analysis. The value of H can be estimated by the slope of $R(l)/S(l)$ versus l on a double logarithmic plot.

The Hurst exponent is a measure of the secular memory of a time series. A value of $H > 0.5$ indicates that the time series exhibits a persistence behavior, namely its trend, whether increasing or decreasing, will remain for a long period of time. A value of $H = 0.5$ implies that the behavior of the time series is a true random walk, where it is equally likely that a decrease or an increase will follow from any particular value. The value of $H < 0.5$ means that the time series exhibits an anti-persistence behavior, namely its trend will likely reverse in the future. More importantly, the Hurst exponent H is directly related to the fractal dimension D of the time series, and the relationship between these two parameters is $D = 2 - H$ (Panchev & Tsekov 2007).

2.3.2 Maximal Lyapunov exponent

A chaotic system is a nonlinear, deterministic system which is usually characterized by fractal structure and sensitivity to small changes in initial conditions. The chaotic properties of an attractor can be quantitatively described by chaotic variables, such as the Lyapunov exponents, the correlation dimension, the Kolmogorov entropy, and so on. The Lyapunov exponent characterizes the rate of separation for two infinite closed trajectories. The divergence of two trajectories with an initial separation δZ_0 in the phase space after time t is

$$|\delta Z(t)| \approx e^{\lambda}t|\delta Z_0|, \tag{5}$$

where λ is the Lyapunov exponent. In principle, the number of Lyapunov exponents is equal to the dimensionality of the phase space. In practice, however, it is often useful to consider the maximal Lyapunov exponent (MLE), because a positive MLE is taken as an indicator of chaos (Wolf et al. 1985). The method for estimating the MLE is defined as (Rosenstein et al. 1993)

$$\lambda = \lim_{t\to\infty} \ln \frac{|\delta Z(t)|}{\delta Z_0}. \tag{6}$$

3 RESULTS

Figure 2 shows the principal component spectrogram for the smoothed monthly-mean of SNs and SAs. From the figure one can see that the plotted line has a negative slope in these two subgraphs, so it is safe to say that these two time series are chaotic signals, not stochastic, noisy signals.

Figure 3 shows the mean mutual information as a function of time delay. The graphs are given for smoothed monthly-mean SNs and SAs. As pointed out by Fraser & Swinney (1986), a reasonable value of the time delay is the value when the mean mutual information exhibits a marked first minimum. From Figure 3 one can see that reasonable values of time delay are 38 for SNs and 39 for SAs. For estimating the embedding dimension of these two indicators, we use the algorithm based on the false nearest neighbor method. From Figure 4 one can see that the curves of $E_2(d)$ for both data sets are not straight lines, implying that these two solar-activity indicators are deterministic signals but not stochastic signals. Moreover, the embedding dimension of both time series is three, suggesting that the long-term solar activity should exhibit the dynamical properties of low-dimensional deterministic chaos.

Figure 5 displays the reconstructed phase spaces with the estimated parameters for SNs and SAs. The phase spaces have been totally unfolded (not like a "ball of wool") and there seem to

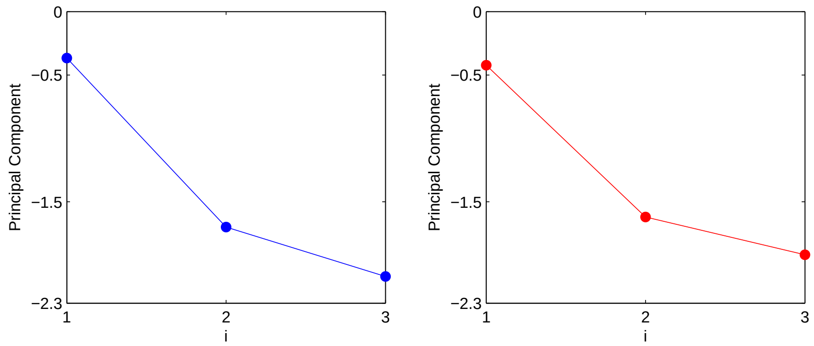

Fig. 2 Plots of the principal component spectrogram for smoothed monthly-mean SNs (*left panel*) and SAs (*right panel*).

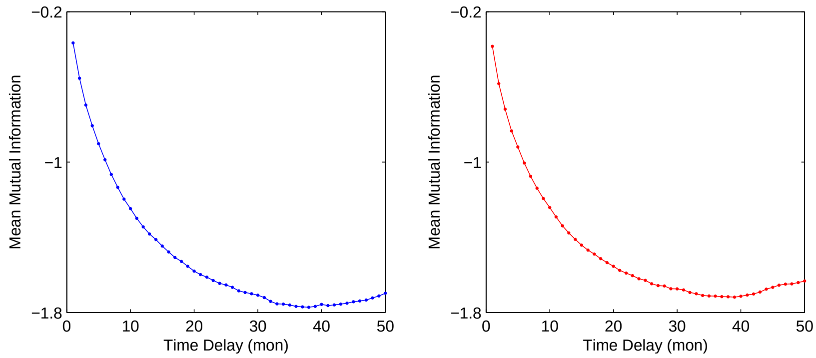

Fig. 3 Plots of mean mutual information as a function of time delay for smoothed monthly-mean SNs (*left panel*) and SAs (*right panel*).

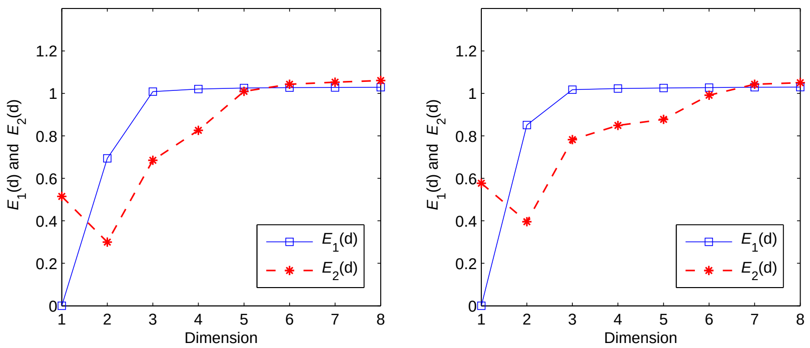

Fig. 4 Plots of the quantities $E_1(d)$ and $E_2(d)$ versus the dimension for smoothed monthly-mean SNs (*left panel*) and SAs (*right panel*).

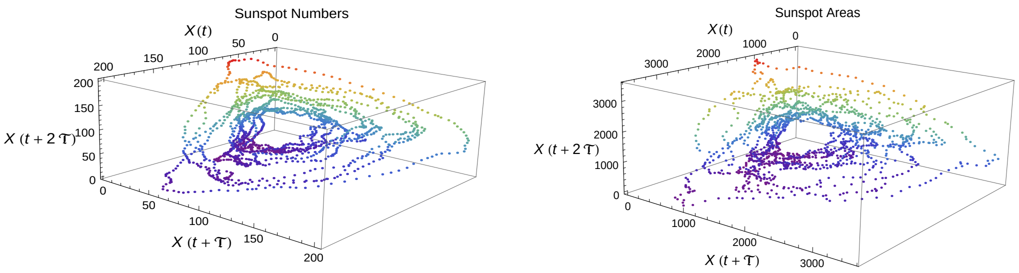

Fig. 5 Plots of reconstructed phase spaces with the estimated parameters for smoothed monthly-mean SNs (*left panel*) and SAs (*right panel*).

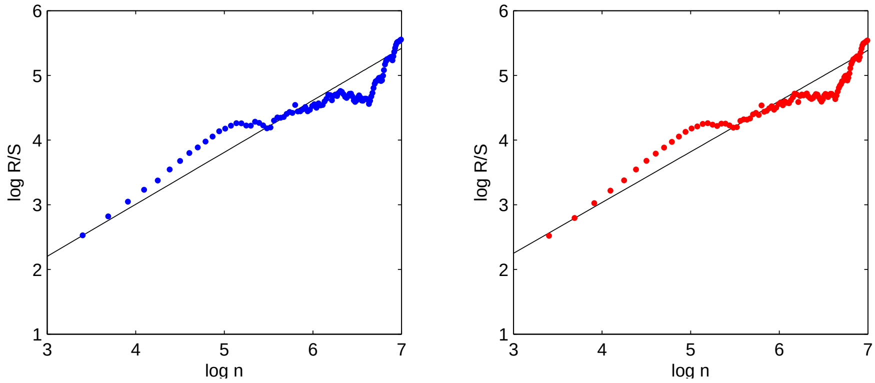

Fig. 6 Rescaled range analysis for smoothed monthly-mean SNs (*left panel*) and SAs (*right panel*).

be some structure underlying these two data sets. The strange attractor characterized by its infinite self-similarity structure is clearly shown in this figure, which is a typical characteristic of a chaotic system. This confirms that the solar activity is governed by low-dimensional dynamics. It should be pointed out that smoothing high-frequency fluctuations helps to recover the dynamic structure of data sets, but this processes cannot inject nonlinear dynamics into the smoothed data (Letellier et al. 2006). Furthermore, comparing the reconstructed phase spaces of SNs and SAs, we see that the dynamics of SAs are more complex than those of SNs. As demonstrated by Carbonell et al. (1994), the larger the fractal dimension, the more chaotic the dynamics of the system. Thus, we infer that the fractal dimension of SAs is larger than that of SNs.

The rescaled range analysis is applied to the smoothed monthly-mean of SNs and SAs, and the results are shown in Figure 6. We can see that the Hurst exponent H is 0.8033 for SNs and 0.7834 for SAs. As the H values of these two time series are in the interval between 0.5 and 1, the fractal motion of solar activity could show long-term persistence on large scales. Subsequently, we calculate the fractal dimension of these two indicators based on the relationship between H and D ($D = 2 - H$), and obtain that the value of fractal dimension is 1.1967 for SNs and 1.2166 for SAs.

Figures 7 and 8 show the divergence and the slope as a function of time for SNs and SAs. The slope of the curves shown as dashed lines in Figure 7 correspond to the theoretical value of MLE. By choosing a reliable range of nonzero values for the slope of the curve to perform straight line fitting, reasonable values of MLE that can be computed are 0.0235 (mon^{-1}) for SNs and 0.0333 (mon^{-1})

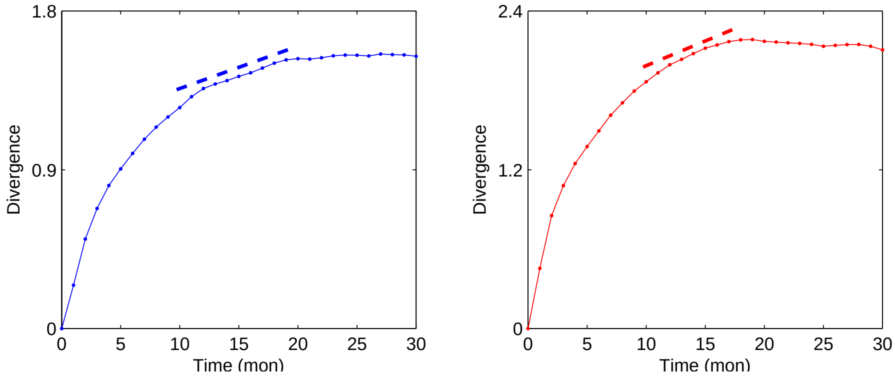

Fig. 7 Plots of divergence as a function of time for smoothed monthly-mean SNs (*left panel*) and SAs (*right panel*).

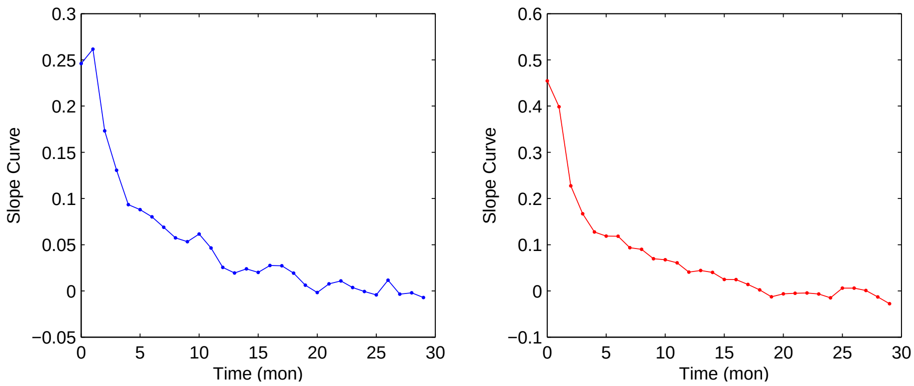

Fig. 8 Plots of the slope curve for smoothed monthly-mean SNs (*left panel*) and SAs (*right panel*).

for SAs. These results suggest that the dynamics underlying the long-term solar activity should be chaotic, and the chaos of SAs is stronger than that of SNs, because of the larger MLE of SAs. The predictability time, defined as $(T_{\rm p} = 1/{\rm MLE})$, is used to describe the length of the strange attractor. In this case, it is about 3.5 years for SNs and about 2.5 years for SAs.

4 CONCLUSIONS AND DISCUSSION

Using the observational data of smoothed monthly-mean SNs and SAs during the time interval of November 1874 to December 2012, we investigate the nonlinear dynamical properties of long-term solar activity. We first filter the time series of SNs and SAs in order to reduce noise and preserve the long-term dynamics of the system. Subsequently, we construct the phase space and calculate the Hurst exponent, maximal Lyapunov exponent, fractal dimension and predictability time. We find that the dynamical behavior of solar activity is governed by a low-dimensional chaotic attractor, whose embedding dimension is three for both data sets. The Hurst exponent indicates that the solar activity has a persistent fractal motion trend, which is consistent with previous studies (Oliver & Ballester

1996; Suyal et al. 2009). Moreover, both the fractal dimension and maximal Lyapunov exponent of SAs are larger than those of SNs, implying that the dynamical system of SAs is more chaotic and complex than SNs. The obtained MLEs and predictions of SNs and SAs indicate that forecasts of solar activity should only be accurate for short- to mid-term behaviors due to complexity that is intrinsic to the system.

Although both SNs and SAs indicate that solar activity is a deterministic chaotic signal with long-term memory, both the fractal dimension and MLE of SAs are larger than those of SNs. Our result seems to support the idea that the dynamical behavior of SAs is more chaotic and complex than SNs. In fact, the SAs have more important physical significance than SNs. Monthly SNs indicate the daily number of sunspots (or sunspot groups) averaged over a month, which is an indication of how frequently the solar dynamo produces solar activities in terms of sunspots. However, the monthly SA gives the daily total area of concentrated magnetic flux of sunspots averaged over a month, which can be viewed as a measure of how powerfully the solar dynamo produces magnetic flux (Li et al. 2005). Therefore, SAs are more complex and realistic for indicating the secular variation of solar activity. In other words, compared to the predictability time that is calculated from SNs, the effective time used for prediction that is obtained from SAs should be more realistic.

Acknowledgements This work is supported by the National Natural Science Foundation of China (Grant No. 61202131) and Chongqing Science and Technology Key Project (cstc2011ggB40027 and cstc2012ggB4004).

References

Cao, L. Y. 1997, Physica D Nonlinear Phenomena, 110, 43
Carbonell, M., Oliver, R., & Ballester, J. L. 1994, A&A, 290, 983
Carr, J. R. 1997, Engineering geology, 48, 269
Charbonneau, P., & Dikpati, M. 2000, ApJ, 543, 1027
Deng, L. H., Qu, Z. Q., Wang, K. R., & Li, X. B. 2012a, Advances in Space Research, 50, 1425
Deng, L. H., Qu, Z. Q., Yan, X. L., Liu, T., & Wang, K. R. 2012b, Journal of Astrophysics and Astronomy, 33, 221
Deng, L., Qi, Z., Dun, G., & Xu, C. 2013a, PASJ, 65, 11
Deng, L.-H., Qu, Z.-Q., Yan, X.-L., & Wang, K.-R. 2013b, RAA (Research in Astronomy and Astrophysics), 13, 104
Deng, L. H., Qu, Z. Q., Liu, T., & Huang, W. J. 2013c, Advances in Space Research, 51, 87
Deng, L. H., Li, B., Zheng, Y. F., & Cheng, X. M. 2013d, New Astron., 23, 1
Feng, S., Deng, L.-H., & Xu, S.-C. 2013, RAA (Research in Astronomy and Astrophysics), 13, 343
Feynman, J., & Gabriel, S. B. 1990, Sol. Phys., 127, 393
Fraser, A. M., & Swinney, H. L. 1986, Phys. Rev. A, 33, 1134
Gong, Y. F., & Xu, J. X. 1997, Signal Processing, 13, 112
Greenkorn, R. A. 2009, Sol. Phys., 255, 301
Hanslmeier, A. 1997, Hvar Observatory Bulletin, 21, 77
Hanslmeier, A., & Brajša, R. 2010, A&A, 509, A5
Hanslmeier, A., Brajša, R., Čalogović, J., et al. 2013, A&A, 550, A6
Hurst, H. E. 1951, Trans. Amer. Soc. Civil Eng., 116, 770
Jevtić, N., Schweitzer, J. S., & Cellucci, C. J. 2001, A&A, 379, 611
Kremliovsky, M. N. 1994, Sol. Phys., 151, 351
Kremlyovskij, M. N., Blinov, A. V., & Chervyakov, T. B. 1992, Soviet Astronomy Letters, 18, 423
Letellier, C., Aguirre, L. A., Maquet, J., & Gilmore, R. 2006, A&A, 449, 379
Li, K. J., Qiu, J., Su, T. W., & Gao, P. X. 2005, ApJ, 621, L81

Li, K. J., Gao, P. X., & Zhan, L. S. 2009, Sol. Phys., 255, 289
Li, Q.-X., & Li, K.-J. 2007a, ChJAA (Chin. J. Astron. Astrophys.), 7, 435
Li, Q.-X., & Li, K.-J. 2007b, PASJ, 59, 983
Mininni, P. D., Gómez, D. O., & Mindlin, G. B. 2002, Physical Review Letters, 89, 061101
Mundt, M. D., Maguire, W. B., II, & Chase, R. R. P. 1991, J. Geophys. Res., 96, 1705
Oliver, R., & Ballester, J. L. 1996, Sol. Phys., 169, 215
Packard, N. H., Crutchfield, J. P., Farmer, J. D., & Shaw, R. S. 1980, Physical Review Letters, 45, 712
Panchev, S., & Tsekov, M. 2007, Journal of Atmospheric and Solar-Terrestrial Physics, 69, 2391
Price, C. P., Prichard, D., & Hogenson, E. A. 1992, J. Geophys. Res., 97, 19113
Rosenstein, M. T., Collins, J. J., & de Luca, C. J. 1993, Physica D Nonlinear Phenomena, 65, 117
Rozelot, J. P. 1995, A&A, 297, L45
Schmalz, S., & Stix, M. 1991, A&A, 245, 654
Suyal, V., Prasad, A., & Singh, H. P. 2009, Sol. Phys., 260, 441
Takens, F. 1981, in Dynamical Systems and Turbulence, Lecture Notes in Mathematics, eds. D. Rand, & L. S. Young (Berlin: Springer Verlag), 898, 366
Tobias, S. M. 1996, A&A, 307, L21
Usoskin, I. G. 2013, Living Reviews in Solar Physics, 10, 1
Wanliss, J. A., & Reynolds, M. A. 2003, Annales Geophysicae, 21, 2025
Wolf, A., Swift, J. B., Swinney, H. L., & Vastano, J. A. 1985, Physica D Nonlinear Phenomena, 16, 285
Zhang, Q. 1998, Sol. Phys., 178, 423